Transp Porous Med (2011) 86:177–198
DOI 10.1007/s11242-010-9615-7

Steady and Unsteady Heat Transfer in a Channel Partially Filled with Porous Media Under Thermal Non-Equilibrium Condition

Pourya Forooghi · Mahdi Abkar · Majid Saffar-Avval

Received: 1 December 2009 / Accepted: 22 June 2010 / Published online: 8 July 2010

Abstract Steady and pulsatile flow and heat transfer in a channel lined with two porous layers subject to constant wall heat flux under local thermal non-equilibrium (LTNE) condition is numerically investigated. To do this, a physical boundary condition in the interface of porous media and clear region of the channel is derived. The objective of this work is, first, to assess the effects of local solid-to-fluid heat transfer (a criterion indicating on departure from local thermal equilibrium (LTE) condition), solid-to-fluid thermal conductivity ratio and porous layer thickness on convective heat transfer in steady condition inside a channel partially filled with porous media; second, to examine the impact of pulsatile flow on heat transfer in the same channel. The effects of LTNE condition and thermal conductivity ratio in pulsatile flow are also briefly discussed. It is observed that Nusselt number inside the channel increases when the problem is tending to LTE condition. Therefore, careless consideration of LTE may lead to overestimation of heat transfer. Solid-to-fluid thermal conductivity ratio is also shown to enhance heat transfer in constant porous media thickness. It is also revealed that an increase in the amplitude of pulsation may result in enhancement of Nusselt number, while Nusselt number has a minimum in a certain frequency for each value of amplitude.

Keywords Local thermal non-equilibrium condition · Porous media · Pulsatile flow · Heat transfer enhancement

List of Symbols

A Amplitude
a_{sf} Specific solid–fluid interface area
Bi Modified Biot number
C_F Forchheimer coefficient

P. Forooghi · M. Abkar · M. Saffar-Avval (✉)
Department of Mechanical Engineering, Amirkabir University of Technology,
P.O. Box 1591-634311, Tehran, Iran
e-mail: mavval@aut.ac.ir

c_p	Specific heat capacity of fluid
Da	Darcy number
d_p	Diameter of particles forming porous medium
e	Thickness of porous layer
f	Frequency
h	Solid-to-fluid heat transfer coefficient
H	Channel's half width
k	Thermal conductivity
K	Permeability
Nu	Nusselt number
p	Pressure
Pr	Prandtl number
Q	Rate of heat transfer
R_{eff}	Ratio of thermal diffusivity
R	Radius of pipe
Re	Reynolds number
T	Dimensional temperature
u	Axial velocity
U	Velocity
x, y	Dimensional coordinates
X, Y	Dimensionless coordinates

Greek symbols

β	Womersley number
ε	Porosity
Φ	Phase lag
γ	Experimental constant
μ	Viscosity
θ	Dimensionless temperature
ρ	Density
σ	Thermal capacity ratio

Subscripts

ave	Time-averaged value
e	Effective value
f	Fluid
in	Inlet
p	Pressure
r	Ratio
s	Solid
S	Steady
sf	Solid-to-fluid ratio
w	Wall
u	Velocity
US	Unsteady
0, m	Mean value

Superscript

* Dimensional variable

1 Introduction

Using porous media inside ducts can dramatically enhance forced convection (Guo et al. 1997; Kaviany 1985). This finding may be a key to improve heat transfer in many industrial applications including optimal design of heat exchangers (Alkam and Al-Nimr 1999; Byun et al. 2006; Klien and Eigenberger 2001; Mohamad 2003), providing an efficient cooling of electronic devices (Huang et al. 2005) and enhancing solar energy storage performance (Nield 1998). There are two approaches to the problem of heat transfer through porous media, namely local thermal equilibrium (LTE) condition and local thermal non-equilibrium (LTNE) condition. In the former, fluid and solid are assumed to be at the same temperature in each point within porous medium, whereas in the latter each phase has its own temperature. Obviously, LTNE is the realistic approach since there is always a temperature difference between fluid and solid which accounts for heat being transferred between them. Concept of LTNE is considered by previous researchers. Al-Nimr and Abu-Hijleh (2002), Abu-Hijleh et al. (2004), Jeng et al. (2006), Khashan et al. (2005), Khashan and Al-Nimr (2006), and Kim and Jang (2002) all have compared the problem under LTE and LTNE conditions, and concluded that LTE condition could applied to some cases but not all. According to Abu-Hijleh et al. (2004), there are five dimensionless parameters controlling the LTE assumption in a transient flow inside a conduit fully filled with porous media, namely volumetric Nusselt number, dimensionless channel's length, the thermal diffusivity ratio, Peclet number, and the solid-to-fluid total thermal capacity ratio. Khashan et al. (2005) showed that the decrease of the Peclet number and the increase of the Biot number (a measure of solid-to-fluid heat transfer) expand the LTE validity over the LTNE region. Moreover, the increase of the effective fluid-to-solid thermal conductivity ratio was found to extend the LTNE region.

The problem of heat transfer in a tube or channel fully filled with porous media is well considered both analytically (Nield 1998; Marafie and Vafai 2001; Nield et al. 2002, 2003; Hooman and Ranjbar-Kani 2004) and numerically (Amiri and Vafai 1994; Jiang et al. 1996; Jiang and Ren 2001; Amiri et al. 1995) with different assumptions regarding to wall boundary condition and consideration of thermal entrance length and thermal dissipation. All above-mentioned studies analyzed heat transfer in a conduit totally filled with porous media. However, filling entire cross-section area of a channel with porous media enhancing heat transfer, may be penalized by considerable amount of pressure drop. In fact, it is more suitable in technological applications to use channels partially filled with porous media. This is a motivation for a lot of researchers to investigate heat transfer in tubes or channels somewhere inside which is mounted a porous insert. For example, Alkam and Al-Nimr (1997), Alkam et al. (2001), and Guo et al. (1997) presented numerical solutions for heat transfer in channels or tubes lined with porous layers, whereas Mohamad (2003) and Pavel and Mohamad (2004) examined a tube with porous media in the core. Huang and Vafai (1994) and Huang et al. (2005) considered heat transfer enhancement due to placing porous blocks on the inner walls of a channel. Al-Nimr and Khadrawi (2003) considered free convection in a vertical channel partially filled with porous media with four different configurations. The present work deals with a channel partially filled with porous media using LTNE condition, unlike the mentioned works which considered the problem under LTE condition. Heat transfer in the presence of pulsatile pressure gradient is also of importance since it can bring about better

understanding of some engineering applications, e.g., heat transfer in ducts, manifolds, and Stirling engines (Guo et al. 1997). Leong and Jin (2005), in their experimental work, stated that presence of porous media enhances heat transfer when flow is pulsatile. Abu-Hijleh et al. (2004) considered LTNE model for transient fluctuating forced convection heat transfer in a channel fully filled with porous media. Khadrawi et al. (2005) solve the problem of pulsatile free convection in a vertical channel. Byun et al. (2006) studied a channel fully filled with porous media under harmonic flow and LTNE condition. Nield and Kuznetsov (2009) and Kuznetsov and Nield (2009) presented analytical solutions for flow and forced convection in channels and tubes filled with porous media under pulsating pressure gradient and studied the effects of frequency on the fluctuating Nusselt number. Unlike all above-mentioned works, that considered fully filled conduits, Guo et al. (1997) solved the problem in a tube partially filled with a porous layer under LTE condition numerically, and reported enhancement of heat transfer in the presence of porous layer.

In this article, steady and pulsatile flow and heat transfer in a channel lined with porous media is numerically investigated under LTNE condition. As the first goal of this work, effects of the three determining parameters, Biot number (a measure of departure from LTE condition), solid-to-fluid thermal conductivity, and porous medium thickness are thoroughly studied in steady flow. Sensibility of Nusselt number to Biot number and thermal conductivity ratio is also briefly studied for pulsatile flow. The second goal is to examine the change in heat transfer when a harmonic term is superimposed on the steady state pressure gradient. The effect of amplitude and frequency of pulsation on Nusselt number are also studied. The main contribution of this article is considering LTNE condition and a partially filled channel at the same time, and introducing a new physical boundary condition in order to close the formulation needed to solve this problem.

2 Mathematical Modeling

Figure 1 is a schematic diagram of the flow field to be shown. A parallel plate channel which is partially filled with porous media is subjected to a constant heat flux boundary condition. The height of the channel is $2H$ and due to symmetry consideration just one-half of the channel is examined. It should be noticed that the following assumptions are considered:

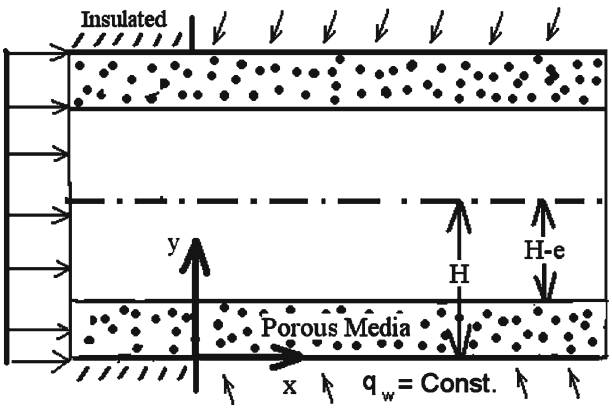

Fig. 1 Schematic diagram of the problem under consideration

- The porous medium is homogeneous, isotropic and in LTNE with the fluid saturating it;
- The thermo physical properties of the fluid and the porous medium are constant;
- The axial conduction effect in the energy equation is negligible;
- The fluid flow and heat transfer conditions are fully developed.

2.1 Governing Equations

To simulate fluid flow inside porous media many researchers have employed Brinkman–Forchheimer-extended Darcy model formulation in their similar works; Jiang and Ren (2001), Mohamad (2003), Alazmi and Vafai (2001, 2002), Khashan et al. (2005) being some examples. According to the Brinkman–Forchheimer-extended Darcy model, the momentum equation for fully developed and unsteady flow can be expressed as

$$\rho_{\mathrm{f}} \frac{\partial u^*}{\partial t^*} = -\frac{\partial p^*}{\partial x} + \mu_{\mathrm{e}} \frac{\partial^2 u^*}{\partial y^2} - \zeta \left(\frac{\mu \cdot u^*}{K} + \frac{\rho_{\mathrm{f}} C_{\mathrm{F}} \varepsilon}{\sqrt{K}} u^{*2} \right), \tag{1}$$

where p^* and u^* are pressure and axial velocity, respectively. By adopting the above formulation, the term u^* refers to the Darcian velocity which is the velocity corresponding to the flow rate. It is assumed that μ_{e} is equal to the intrinsic viscosity of the fluid (μ), as done in many references.

The pulsating pressure gradient is given as

$$-\frac{\partial p^*}{\partial x} = -\left(\frac{\partial p^*}{\partial x} \right)_{\mathrm{s}} \left[1 + A_{\mathrm{p}} \sin \left(2\pi \cdot f \cdot t^* \right) \right], \tag{2}$$

where A_{p} is the amplitude of pulsation and f is the pulsation frequency. A_{p} is equal to zero when flow is steady.

Also, energy equations of fluid and solid phases in the case of the LTE condition are as follows (Byun et al. 2006).

Fluid phase energy:

$$\varepsilon \rho_{\mathrm{f}} c_{\mathrm{pf}} \frac{\partial T_{\mathrm{f}}}{\partial t^*} + \rho_{\mathrm{f}} c_{\mathrm{pf}} \frac{\partial}{\partial x} \left(u^* T_{\mathrm{f}} \right) = \varepsilon k_{\mathrm{f}} \left(\frac{\partial^2 T_{\mathrm{f}}}{\partial y^2} \right) + \zeta \left(h \cdot a_{\mathrm{sf}} \left(T_{\mathrm{s}} - T_{\mathrm{f}} \right) \right) \tag{3}$$

Solid phase energy:

$$(1 - \varepsilon) \rho_{\mathrm{s}} c_{\mathrm{ps}} \frac{\partial T_{\mathrm{s}}}{\partial t^*} = (1 - \varepsilon) k_{\mathrm{s}} \left(\frac{\partial^2 T_{\mathrm{s}}}{\partial y^2} \right) - h \cdot a_{\mathrm{sf}} \left(T_{\mathrm{s}} - T_{\mathrm{f}} \right) \tag{4}$$

h stands for the fluid-to-solid heat transfer coefficient and a_{sf} is the surface area per unit volume of a porous medium. Amiri and Vafai (1994) presented the expressions for these parameters as follows:

$$h = \frac{k_{\mathrm{f}}}{d_{\mathrm{p}}} \left[2 + 1.1 \cdot Pr^{1/3} \left(Re \frac{d_{\mathrm{p}}}{2H} \right)^{0.6} \right] \tag{5}$$

$$a_{\mathrm{sf}} = \frac{6 \cdot (1 - \varepsilon)}{d_{\mathrm{p}}} \tag{6}$$

The above formulations are applicable to both fluid and porous regions; the fluid occupied region is identified by setting the index $\zeta = 0$ and the porous region marked by $\zeta = 1$.

Using the following dimensionless parameters and variables

$$X, Y = \frac{x, y}{2H}, \quad P = \frac{p^*}{\rho_f U_0^2}, \quad u = \frac{u^*}{U_0}, \quad t = \frac{t^*}{\left(\frac{2H}{U_0}\right)}, \quad \theta_{f,s} = \frac{T_{f,s}}{\frac{q_w(2H)}{k_f}}$$
$$Re = \frac{\rho_f U_0 (2H)}{\mu}, \quad Da = \frac{K}{(2H)^2}, \quad k_{sf} = \frac{k_s}{k_f}, \quad Bi = \frac{h a_{sf} (2H)^2}{k_f},$$
$$\mu_r = \frac{\mu_e}{\mu}, \quad \sigma = \frac{\rho_s c_{ps}}{\rho_f c_{pf}}$$

Equations 1–4 can be rewritten in their non-dimensional forms, neglecting the effect of axial conduction.

Non-dimensional momentum equation:

$$\frac{\partial u}{\partial t} = -\frac{\partial P}{\partial X} + \frac{\mu_r}{Re}\frac{\partial^2 u}{\partial Y^2} - \zeta\left(\frac{u}{ReDa} + \frac{C_F \varepsilon}{\sqrt{Da}} u^2\right) \tag{7}$$

Non-dimensional pressure gradient:

$$-\frac{\partial P}{\partial X} = -\left(\frac{\partial P}{\partial X}\right)_s \left[1 + A_p \sin\left(\frac{2\beta^2}{Re} t\right)\right], \tag{8}$$

where β is Womersley number and defined as

$$\beta = H\sqrt{\frac{2\pi \cdot f}{\nu}} \tag{9}$$

Non-dimensional fluid phase energy:

$$\varepsilon\frac{\partial \theta_f}{\partial t} + u\frac{\partial \theta_f}{\partial X} = \varepsilon\frac{1}{RePr}\left(\frac{\partial^2 \theta_f}{\partial Y^2}\right) + \zeta\left(\frac{Bi}{RePr}(\theta_s - \theta_f)\right) \tag{10}$$

Non-dimensional solid phase energy:

$$(1-\varepsilon)\sigma\frac{\partial \theta_s}{\partial t} = (1-\varepsilon)k_{sf}\frac{1}{RePr}\left(\frac{\partial^2 \theta_s}{\partial Y^2}\right) - \frac{Bi}{RePr}(\theta_s - \theta_f) \tag{11}$$

To solve the above system of equations Chatwin's approximation is employed (Chatwin 1975) i.e.

$$\frac{\partial \theta_f}{\partial X} = \frac{2}{RePr} \tag{12}$$

The term Bi stands for modified Biot number which shows heat transfer between fluid and solid phases within the porous insert and can be expressed in terms of porous media parameters by replacing from Eqs. 5 and 6:

$$Bi = 6 \cdot (1-\varepsilon) \cdot \left(\frac{2H}{d_p}\right)^2 \cdot \left[2 + 1.1 \cdot Pr^{1/3}\left(Re \cdot \left(\frac{d_p}{2H}\right)\right)^{0.6}\right] \tag{13}$$

2.2 Boundary Conditions

No-slip and LTE assumptions are exerted on the channel walls. In fact, the channel wall is the only place where fluid and solid have enough time to reach the thermal equilibrium, and are essentially isothermal subsequently.

$$\begin{cases} u = 0 \\ \theta_s = \theta_f \end{cases} \quad \text{at} \quad Y = 0 \tag{14}$$

The heat flux on the wall is divided into two parts: fluxes of heat through solid and fluid phases. According to Alazmi and Vafai (2002) the heat flux boundary condition on the wall could be stated as:

$$q_w = [\varepsilon + (1-\varepsilon)k_s] \cdot \frac{\partial T_f}{\partial Y} \quad \text{at } Y = 0 \tag{15}$$

Or, in dimensionless form:

$$\frac{\partial \theta_f}{\partial Y} = [\varepsilon + (1-\varepsilon)k_{sf}]^{-1} \quad \text{at } Y = 0 \tag{16}$$

Also, symmetry condition at the center of the channel can be written as:

$$\frac{\partial u}{\partial Y} = \frac{\partial \theta_f}{\partial Y} = 0 \quad \text{at } Y = 0.5 \tag{17}$$

Another representation of boundary condition is found by noting the following.

It is also needed to employ suitable boundary condition at the interface between clear fluid and porous media. One of the most cited expressions for hydrodynamic boundary conditions at this interface is the experimental formula presented by Beavers and Joseph (1967):

$$\left.\frac{du}{dy}\right|_{\text{Interface}} = \frac{\gamma}{K}(u|_{\text{Interface}} - u_{f,\text{mean}}) \tag{18}$$

where u and u_f stand for velocities in clear fluid and porous media, respectively, and the index *mean* indicates on area average. γ is an experimental constant. However, Eq. 18 is not appropriate for being used in a CFD code since it deals with average quantities. Alazmi and Vafai (2001) did a comprehensive survey on hydrodynamic and thermal boundary interface conditions, and present a list of mathematical formulas for them. In the present work, boundary conditions number 2 in Table 1 of Alazmi and Vafai (2001) are adopted being, with notation used in this article:

$$\begin{aligned} u &= u_f \quad \text{at } Y = e/H \\ \frac{\partial u}{\partial Y} &= \mu_r \frac{\partial u_f}{\partial Y} \quad \text{at } Y = e/H \end{aligned} \tag{19}$$

For thermal boundary condition, however, the relations presented in Alazmi and Vafai (2001) failed since they only investigated the problem under LTE condition. To the knowledge

Table 1 Mesh independency of results; Case 1: $Bi = 10{,}000$, $k_{sf} = 1$, $e/2H = 0.2$, Case 2: $Bi = 10{,}000$, $k_{sf} = 100$, $e/2H = 0.2$

Number of nodes	Nusselt number (case 1)	Nusselt number (case 2)
110	5.67	11.80
100	5.67	11.80
90	5.67	11.79
70	5.65	11.73

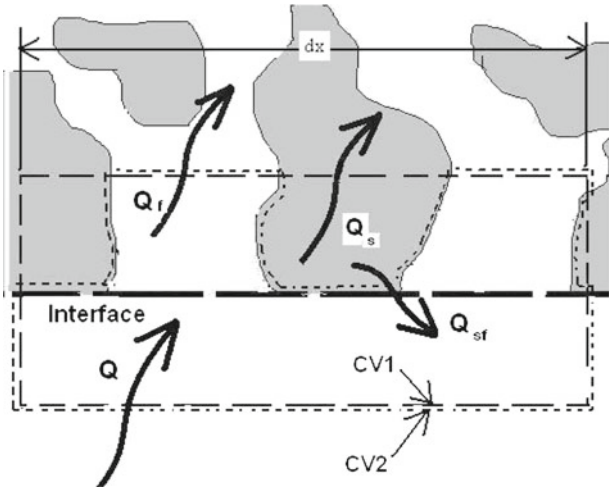

Fig. 2 Schematic diagram of interface boundary condition

of authors, there is no thermal interface boundary condition for LTNE condition in the open literature. The difference between the two cases is clear: for LTE condition fluid and solid temperatures in porous media, say θ_f and θ_s, respectively, are equal; whereas for LTNE this identity is not valid, so another equation is needed in order to close the problem.

In the present work, a physical interface boundary condition is introduced. According to Fig. 2 a thin control volume (CV1) is being examined. The thickness of the control volume is infinitesimally small so that heat fluxes crossing the vertical boundaries of the CV1 are negligible. The heat flux Q enters the CV1 from the lower surface via fluid, and goes out through the upper surface via both fluid and solid, with the rates Q_f and Q_s, the heat balance is:

$$Q = Q_f + Q_s \tag{20}$$

Since the proportion of fluid surface area to overall surface area in the interface is ε, for an isotropic and homogenous porous media, Eq. 20 can be rewritten, in dimensionless form, as Eq. 21:

$$\frac{\partial \theta}{\partial Y} = \varepsilon \frac{\partial \theta_f}{\partial Y} + (1-\varepsilon) k_{sf} \frac{\partial \theta_s}{\partial Y} \quad \text{at } Y = e/H \tag{21}$$

Equation 21 is the same as boundary condition I in the work of Alazmi and Vafai (2001) in case $\theta_s = \theta_f$. It is also evident that fluid temperature at the interface should be continues, so another boundary condition at this point is

$$\theta = \theta_f \quad \text{at } Y = e/H \tag{22}$$

To close the problem still one equation is absent. To find it, one can consider a control volume which contains only fluid phase in the porous media. In other words, the control volume CV2 is obtained by omitting solid phase in the upper part of CV1, as shown in Fig. 2. This time, there are three heat fluxes crossing the control volume boundaries: the heat entering from clear fluid (Q), the heat going out to fluid in porous media (Q_f), and the heat transfer taking place between the two phases (Q_{sf}). The arrows in Fig. 2 indicate on flux directions. The equation of heat balance in CV2 is:

$$Q = Q_{sf} + Q_f \tag{23}$$

The key is that Q_{sf} must be calculated in the same manner as done within a porous medium, i.e., Q_{sf} equals heat transfer coefficient h multiplied by fluid–solid surface area multiplied by temperature difference $(T_s - T_f)$. The fluid–solid surface area inside CV2 is comprised of two parts: the surface area within porous medium and the surface area at the interface of clear fluid and porous medium. As CV2 is infinitesimally thin, the former is negligible, so the fluid-to-solid heat transfer surface area in CV2 could be approximated by $(1-\varepsilon)\cdot \mathrm{d}x$. Thus,

$$Q_{sf} = h \cdot (1-\varepsilon) \cdot \mathrm{d}x \cdot (T_s - T_f) \tag{24}$$

By combining Eqs. 23 and 24 and considering the definition of Biot number it could be stated that:

$$\frac{\partial \theta}{\partial Y} = \frac{Bi}{a_{sf}(2H)} \cdot (1-\varepsilon) \cdot (\theta_s - \theta_f) + \varepsilon \cdot \frac{\partial \theta_f}{\partial Y} \tag{25}$$

Equations 21, 22, and 25 form the set of equations required for finding the three unknowns θ, θ_f, and θ_s. It could be kept in mind that the heat transfer coefficient h could be different inside porous media and on the interface; therefore, a more general formulation could be obtained by defining two different Biot numbers in Eqs. 11 and 25; however, in this work both Biot numbers assumed to be equal. This assumption is justifiable since the fluid velocity on the interface is very close to that of porous region. By adding Eq. 25 to Eq. 21 a forth equation is obtained which, though is not independent, can provide insight:

$$(1-\varepsilon) \cdot k_{sf} \cdot \frac{\partial \theta_s}{\partial Y} = \frac{Bi}{a_{sf}(2H)} \cdot (1-\varepsilon) \cdot (\theta_s - \theta_f) \tag{26}$$

When Biot number is zero, i.e., there is no heat transfer from fluid to solid, Eq. 26 expresses that the heat transfer via solid phase at the interface is zero. In other words, when Biot number is zero contribution of solid phase in heat transfer vanishes both within the porous media and at the interface. The other asymptotic condition is when Biot is very large, which correspond to LTE condition. In this case, the right-hand side of the Eq. 26 will be infinite unless solid-to-fluid temperature difference tends to zero. This result is compatible with the assumption of thermal equilibrium.

Replacing a_{sf} from Eq. 6, Eq. 25 can be more simplified:

$$\frac{\partial \theta}{\partial Y} = \frac{Bi}{6\left(2H/d_p\right)} \cdot (\theta_s - \theta_f) + \varepsilon \cdot \frac{\partial \theta_f}{\partial Y} \tag{27}$$

It is shown in the previous subsection that Biot number and $2H/d_p$ can be expressed as functions of each other; therefore, only one of them may be regarded as the independent parameter. In this article, parametric study is performed on Biot number. Corresponding values of $2H/d_p$ are calculated by solving Eq. 13 numerically. In constant Reynolds and Prandtl numbers and porosity Eq. 27 can be rewritten as:

$$\frac{\partial \theta}{\partial Y} = F(Bi) \cdot (\theta_s - \theta_f) + \varepsilon \cdot \frac{\partial \theta_f}{\partial Y} \tag{28}$$

in which F is an increasing function of Biot number. It is worth adding that as the ratio of H to d_p could not have every arbitrary value in reality, Biot number also cannot be selected without enough care. For example, as could be calculated, if Biot is $< 1{,}000$, it will mean that $2H/d_p$ is of order 5 or less, and it is not acceptable in physical sense. Hence, Biot number has to be greater than roughly 3,000 in this case. However, as Biot number depends on other parameters like Reynolds and Prandtl number plus porosity, it is possible for Biot number to

be of lower values in other cases. It should be added that Eq. 13 is not a general formula and can be different for different types of porous media than that examined by Amiri and Vafai (1994).

3 Numerical Solution

Equations are numerically solved using a finite-difference scheme. The central difference is used in order to discrete derivatives in diffusion terms. The flow is assumed to be quasi-dynamically and thermally fully developed the same assumptions as adopted by Guo et al. (1997). In order to accurately handle the problem it is necessary for the mesh width to be small enough near the wall for small values of porous thicknesses. A non-uniform logarithmic grid is used for the transverse coordinate. All the calculations are performed with meshes guaranteeing grid-independent results with 100 nodes in the span-wise direction. The mesh independency of the solution is shown in Table 1. The discretized equations are solved by marching in time. The first order and second order approximations are used in order to discretize temporal and spatial derivatives, respectively. For analyzing pulsating flow, the solution for the corresponding steady non-pulsating flow is used as the initial condition to reduce the computational time, and time marching is stopped as the solution reaches a dynamic steady state (in which similar patterns are repeated in successive periods of pulsation.).

4 Results and Discussion

4.1 Steady Flow

It is a crucial task in this survey to define a meaningful Nusselt number which indicates on total amount of heat transfer per degree of temperature difference between bulk of fluid and channel's wall. It is especially important to make this ratio non-dimensionalized with a suitable thermal conductivity. It seems most sensible to use thermal conductivity of fluid in the definition of Nu since one of the aims of the present study is to assess the effect of different solid materials on overall heat transfer. Hence, Nusselt number is defined as:

$$Nu_{\mathrm{S}} = \frac{h\,(2H)}{k_{\mathrm{f}}} = \frac{q_{\mathrm{w}}\,(2H)}{(T_{\mathrm{w}} - T_{\mathrm{b}})\,k_{\mathrm{f}}} = \frac{1}{(\theta_{\mathrm{w}} - \theta_{\mathrm{b}})}, \tag{29}$$

where θ_{w} and θ_{b} stand for wall and bulk temperature, respectively:

$$\theta_{\mathrm{b}} = 2\int_{0}^{0.5} u\theta_{\mathrm{f}}\mathrm{d}Y \tag{30}$$

The term Nu_{S} indicates "steady state" Nusselt number.

Figure 3 shows steady flow profiles in different porous thicknesses. When the non-dimensional thickness is smaller than roughly 0.4, almost entire flow passes through clear region and the velocity in porous region is nearly zero. As the width of clear region decreases, due to high pressure gradient resulted from frictional losses, flow begins to go into porous media. In the case of the channel fully filled with porous media, profile shape suddenly changes, and becomes similar to that of a slug flow. As shown later, these flow patterns highly affect the heat transfer in the channel.

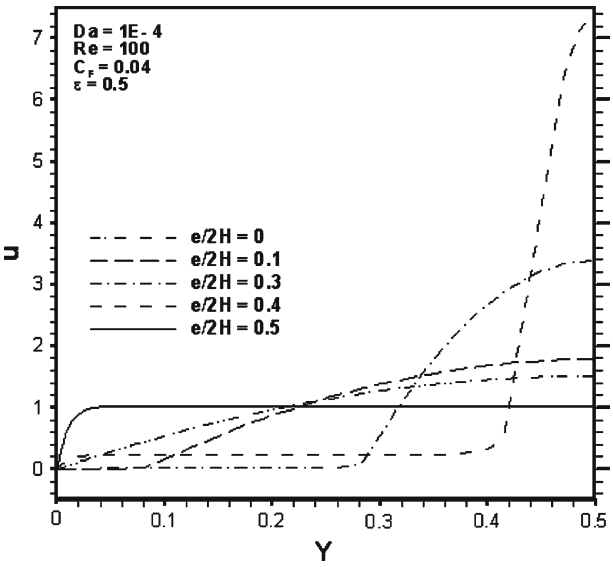

Fig. 3 Flow profiles in different values of $e/2H$

It is worth emphasizing that in the present work the pressure gradient is adjusted so that the normalized mean fluid velocity is equal to 1 for all porous media thicknesses.

As mentioned before, it is admitted that mounting of porous inserts inside a channel could improve heat transfer, however, it impose some extra cost because of considerable pressure drop. Thus, unsuitable use of porous media in a channel may be penalized with high energy losses. Figure 4 shows variation of pressure drop with porous media thickness in two different Darcy numbers. The pressure drops in this figure are normalized with the pressure drop corresponding to a clear channel. It is easily seen that when porous media occupy more than roughly half of the channel, pressure drop increases sharply. The effect of Darcy number is more significant in larger thicknesses.

In order to validate the present solution of energy equation, Nusselt numbers obtained from numerical code are compared with those reported by Guo et al. (1997) in Table 2. They solved the problem of convective heat transfer in a tube lined with porous media under LTE condition therefore the results are presented for different values of e/R instead of $e/2H$. In order to reach LTE condition in the present code, Biot number set to 10^7, a large value nearly corresponding to LTE condition, as it will shown later in this section. It must be mentioned here that the validation of the present solution for momentum equation will be verified in Sect. 4.2.

Variation of Nusselt number against porous layer thickness is plotted in Figs. 7 and 8, in different values of Bi and k_{sf}.

Although in real applications $k_{\mathrm{sf}} = 1$ is not common, it can provide insight in a scientific survey as for some other researches (Alkam et al. 2001; Mohamad 2003; Guo et al. 1997). It is observed that when the thermal conductivity ratio equals 1, the trend of Nusselt number is not monotonic. It is shown, in Fig. 7, that Nusselt number decrease as $e/2H$ increases before reaching 0.4, then Nusselt number surges and reaches its greatest value at $e/2H = 0.5$. It means that a channel fully filled with porous media has the largest heat transfer coefficient. This trend can be explained by considering Fig. 3—velocity profiles. When $e/2H$ is low,

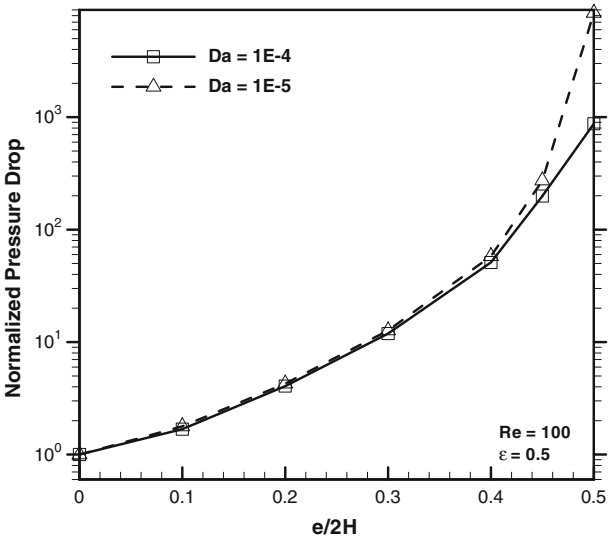

Fig. 4 Variation of pressure drop with porous media thickness in $Da = 10^{-4}, 10^{-5}$

Table 2 Comparison of Nusselt number in the present work with Guo et al. (1997); $Re = 50$, $Da = 10^{-4}$, $\varepsilon = 0.6$, $k_{sf} = 10$; $Bi = 10^7$ for the present work

e/R	Present work	Guo et al. (1997)
0	4.34	4.34
0.2	4.24	4.27
0.4	4.17	4.04
0.6	4.10	4.22
0.8	8.25	8.60
1	75.01	75.32

there is a region of still fluid adjacent to the channel's wall, which act as an impediment to heat transfer from the wall. Its effect is to some degree similar to a thickened laminar boundary layer which reduces forced convection. As the value of $e/2H$ become close to 0.5, flow start going through porous media, and it leads to increase in Nusselt number. In the case of a channel fully filled with porous media, the slug flow pattern is obtained, as discussed earlier. It is well-known that Nusselt number dramatically enhances in a slug flow (Bejan 1984) and the same is observed in Fig. 5.

To add the effect of thermal conductivity of solid phase to previous discussion, Fig. 6 is presented, in which all parameters set as of Fig. 5, except k_{sf} that is equal to 100. As expected, using a more conductive material can enhance Nusselt number. Thanks to suitable definition of Nusselt number this intuitional result can be seen clearly in Fig. 6. Although the effect of flow profiles is either present in this case, this effect is overcome by the effect of high thermal conductivity. In other words, using a more conductive material in porous media reduces conductive resistance to heat transfer, and leads to an increase in Nusselt number, even though effect of porous media on flow profile still tends to reduce heat transfer. As porous media fill almost the whole cross-section area, the both effects are in the same direction, and it brings about a sharp increase in Nusselt number. The trends observed in Figs. 5 and 6 are repeated in some other researches (Alkam et al. 2001; Guo et al. 1997); however,

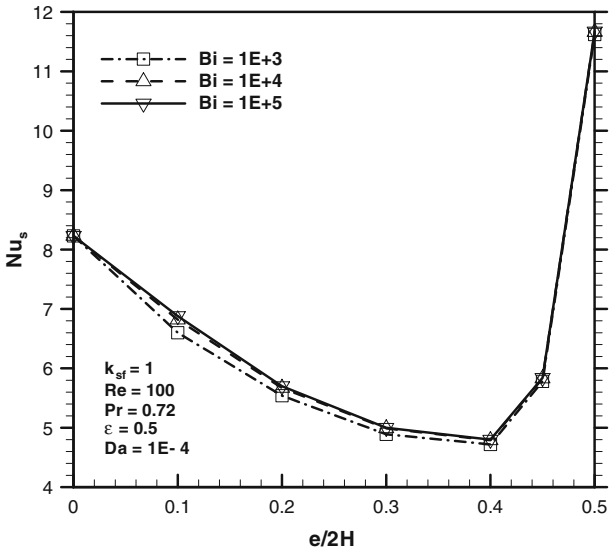

Fig. 5 Variation of Nusselt number with porous layer thickness in three Biot numbers; $k_{\mathrm{sf}} = 1$ and $Da = 10^{-4}$

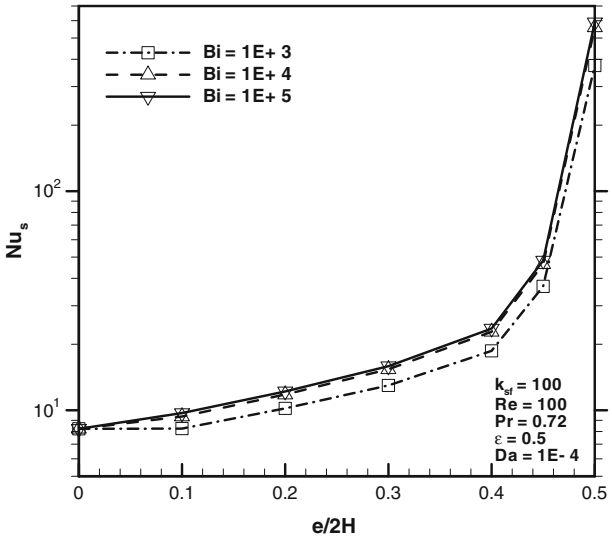

Fig. 6 Variation of Nusselt number with porous layer thickness in three Biot numbers; $k_{\mathrm{sf}} = 100$ and $Da = 10^{-4}$

the results are quantitatively different because Alkam et al. (2001) investigated the problem with constant wall temperature, and Guo et al. (1997) focused on a tube rather than a channel.

Another trend found in Figs. 5 and 6 is that Nusselt number increases with Biot number. This may be better observed in Fig. 7, where variation of Nusselt number with Biot number is plotted in different values of k_{sf} and $e/2H$. Biot number varies between 10^3 and 10^6. As observed earlier, Nusselt number increases with Biot number. It is not difficult to justify this

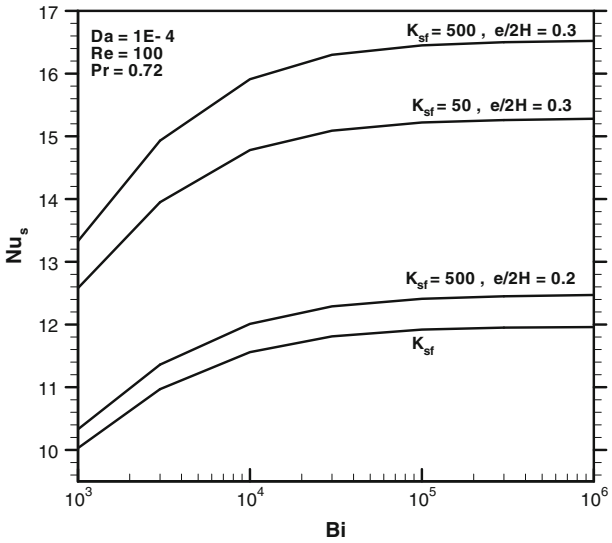

Fig. 7 Variation of Nusselt number with Biot number in different values of k_{sf} and $e/2H$

trend, since Biot number is a measure of fluid-to-solid heat transfer, a criterion whose value indicates on LTE. In other words, as Bi increases, the problem becomes more close to LTE condition and vice versa. In fact, when Biot number decreases, contribution of solid phase in heat transfer becomes lower. In very low values of Bi, there is almost no exchange between two phases, so fluid phase is responsible for the whole heat transfer while the isolated solid occupies half of the area. It obviously decreases heat transfer. As Bi becomes close to 10^6, all curves plateaued. It can be interpreted as reaching LTE condition, above this Biot number. A useful inference of this figure is that with taking LTE condition for granted, overestimation of Nuselt number is unavoidable; however, when Bi is enough close to a certain value corresponding to LTE (in the present case, 10^6) the error is not considerable, but it must be examined before taking LTE assumption. In Fig. 7, for $k_{\mathrm{sf}} = 500$ and $e/2H = 0.3$, this error, when Bi equals 10^5, is some 0.5%, and for $Bi = 3 \times 10^4$ and 10^4 is 1.5 and 4%, respectively. The error increases considerably as Biot number become smaller.

To better show that increment of Biot number leads to LTE condition, solid-to-fluid temperature difference within porous layer is depicted in Fig. 8. It is obvious that the more the Biot number is, the less temperature difference is resulted. Temperature differences are greater near the porous–clear interface since two phases are almost at rest near the channel's wall, and it provide enough time for reaching LTE to some extent. It must be noted that without adopting suitable boundary condition at the interface it would be impossible to obtain correct results in problems like this.

The last figure in this subsection is Fig. 9 indicating on increase of Nusselt number with k_{sf}. The effect of Darcy number is also examined in this plot, which is proven not to be significant over the range of 10^{-4} to 10^{-5}. Although effect of thermal conductivity is clear in the three Figs. 5, 6 and 7, Fig. 9 aims to investigate this effect directly and in a wider range. It is clear that increasing thermal conductivity of solid phase augments Nusselt number, but the rate of this increase decreases when k_{sf} becomes greater than roughly 100. This result could be important because higher values of k_{sf} resulted in the numerical difficulties and to

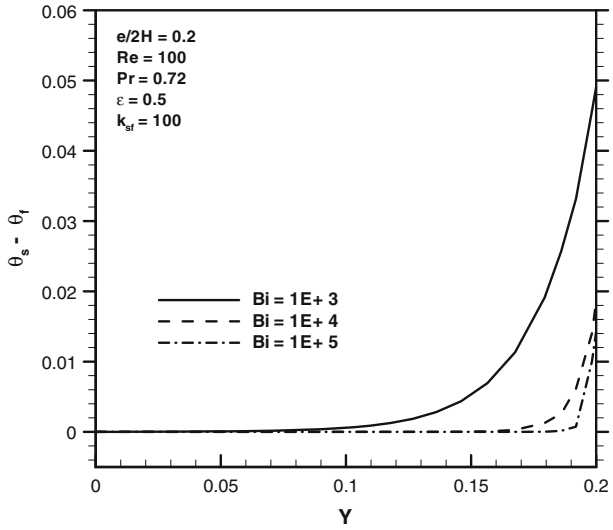

Fig. 8 Solid-to-fluid temperature difference within porous layer in $Bi = 10^3, 10^4, 10^5$; $k_{\mathrm{sf}} = 100$ and $e/2H = 0.2$

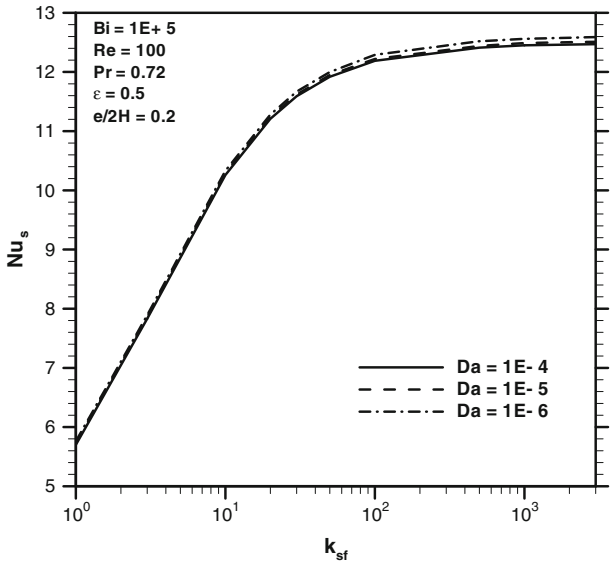

Fig. 9 Variation of Nusselt number with solid-to-fluid thermal conductivity ratio; $Da = 10^{-4}, 10^{-5}$; $Bi = 10^5$ and $e/2H = 0.2$

avoid this, more computational cost is needed. When k_{sf} is smaller than 10, Nu is nearly a linear function of logarithm of k_{sf}.

4.2 Pulsating Flow

When a pressure gradient in the form of Eq. 8 is applied, fluid velocity in each point can be expressed as a harmonic term superimposed on the steady velocity corresponding to

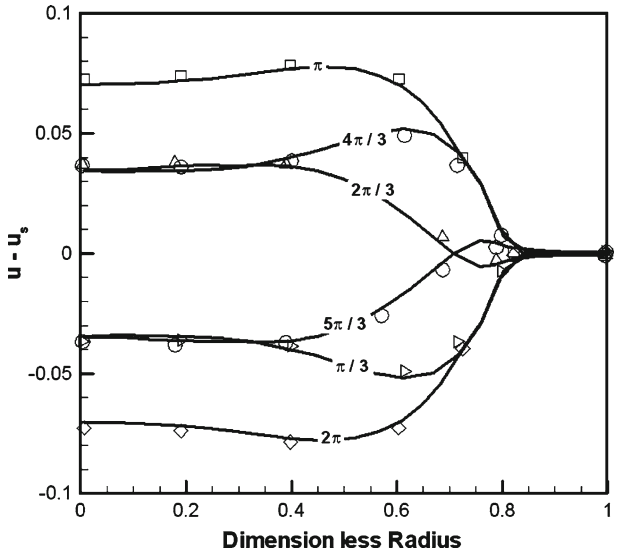

Fig. 10 Comparison of velocity profiles in different times in a period in the present work (*symbols*) with Guo et al. (1997); $Re = 100$, $C_F = 0.057$, $A_p = 0.9$, and $\beta = 10$

$(\partial P/\partial X)_s$. In fact, the flow is a steady harmonic flow since the transition from still fluid is not considered. Evidently, mean velocity is a function of time in the form of:

$$u_m = u_{m,S}\left[1 + A_u \sin\left(\frac{2\beta^2}{Re}t + \Phi\right)\right], \tag{31}$$

where $u_{m,S}$ stands for mean velocity in steady flow corresponding to average pressure gradient, A_u and Φ are amplitude and phase lag of mean velocity pulsation, respectively. Both A_u and Φ are functions of A_p and frequency or β. In the case of very small frequency, A_p tends to A_u and Φ vanishes. As frequency increases, A_p decreases and Φ grows. As this work deals with time-averaged quantities the phase lag is not paid more attention. However, amplitude of flow pulsation is an important parameter since it certainly influences the heat transfer coefficient. It is worth emphasizing that not two flows with same A_u are alike because A_u only indicates on amplitude of mean flow, and flow profiles are different in different values of frequency or β.

Figure 10 shows velocity profiles in six different times during a period of pulsation obtained from the present work and the work of Guo et al. (1997). In order to verify the present results for energy equation in unsteady condition, they are also compared, in Table 3, with those of Guo et al. (1997) for flow in pipes. A little change in governing equations is needed to deal with the problem for pipes, which avoided to be mentioned for the sake of briefness. In the work of Guo et al. the ratio of thermal conductivity due to pulsation, R_{eff}, is defined as:

$$R_{eff} = \frac{\int_0^{(\pi\cdot Re)/\beta^2}\int_0^{0.5}(\theta-\theta_S)(u-u_S)r\cdot dr\cdot dt}{\int_0^{0.5}u_S r\cdot dr\cdot dt}\cdot(Re\cdot Pr)^2/8 \tag{32}$$

Table 3 Comparison of thermal conductivity ratio in present work with Guo et al. (1997); $Re = 50$, $\varepsilon = 0.6$, $k_{sf} = 10$, $A_p = 0.9$, $\beta = 1$, and $Bi = 10^7$ for present work

e/R	Present work	Guo et al. (1997)
0	236.1	236.2
0.2	720.6	733.3
0.4	1387.4	1408.4
0.6	1973.0	2002.3
0.8	1138.3	1142.5
1.0	44.8	46.5

As mentioned before, index s indicates on variables in steady flow with the same average pressure gradient. Variation of R_{eff} against porous layer thickness obtained from the present work and Guo e al. (2007) is presented in Table 3.

A major difficulty in the analysis of heat transfer in pulsating flows is adopting a sensible definition for bulk temperature which is essential for calculating average Nusselt number. The problem is arisen especially in large amplitudes, which may lead to reverse flows. Guo and Sung (1997) examined some definitions of average Nusselt number for a pulsatile flow. Their work reveals that using inappropriate definitions for average Nusselt number, e.g., using Eq. 29 for calculating time-dependent Nusselt number then averaging over a period, results in insensible trends in Nusselt number. Therefore, Guo and Sung (1997) proposed an improved version of Nusselt number which shows better agreement with experimental results:

$$Nu_{\text{US}} = \frac{1}{\theta_{\text{w}} - \theta_{\text{b,US}}} \tag{33}$$

where $\theta_{\text{b,US}}$ is defined as:

$$\theta_{\text{b,US}} = \frac{\int_0^{0.5} \theta_{\text{f}} \sqrt{u^2}\,\text{d}Y}{\int_0^{0.5} \sqrt{u^2}\,\text{d}Y} \tag{34}$$

$$Nu_{\text{ave}} = \frac{\int_0^{(\pi \cdot Re)/\beta^2} Nu_{\text{US}} \cdot \text{d}t}{\int_0^{(\pi \cdot Re)/\beta^2} \text{d}t} \tag{35}$$

In the present work, Eq. 35 is used to calculate average Nusselt number for pulsatile flow. In order to assess the impact of flow pulsation amplitude on average Nusselt number, Fig. 11 is plotted. Instead of Nu_{ave}, its normalized value is presented to better compare its value in different conditions. It should be noted that for unsteady heat transfer an additional parameter, σ, must be considered. To avoid unnecessary complication, in this section σ is considered to be equal to 0.6, corresponding to heat capacity ratio of water and aluminum. Biot number is also set to the sensible value of 10^5.

It is observed that Nusselt number in pulsatile flow is greater than that of steady flow almost in all conditions; however, its trend is not monotonic regarding to both frequency (or Womersley number) and amplitude. In smaller Womersley numbers, average Nusselt number increases constantly with the amplitude, but in greater Womersley numbers, average Nusselt

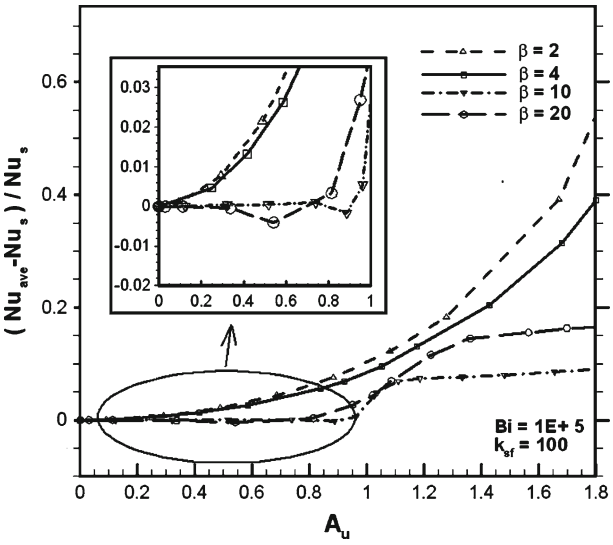

Fig. 11 Variation of normalized pulsatile average Nusselt number with the amplitude of flow pulsation in different Womersley numbers; $Pr = 1.5, \sigma = 0.6, Bi = 10^5, e/2H = 0.2$, and $k_{\mathrm{sf}} = 100$

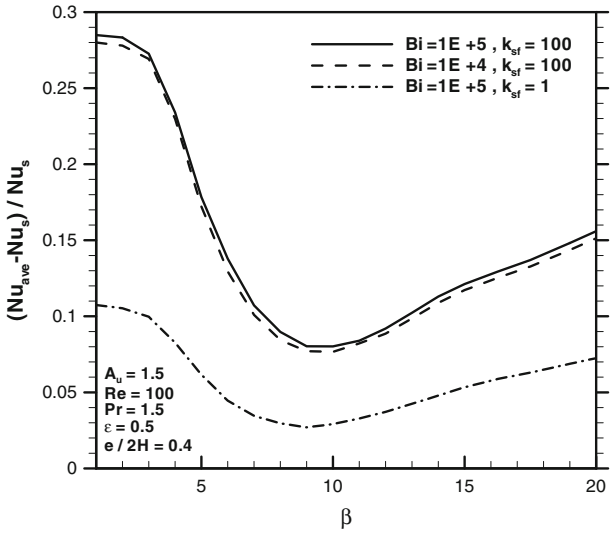

Fig. 12 Variation of normalized pulsatile average Nusselt number with Womersley number in different values of Biot number and k_{sf}; $Pr = 1.5, \sigma = 0.6, e/2H = 0.2$, and $A_{\mathrm{u}} = 1.5$

number remains nearly constant when A_{u} is smaller than roughly one, and even becomes negative somewhere near $A_{\mathrm{u}} = 1$. However, a sharp increase in Nusselt number is observed when A_{u} is slightly more than unity. The same qualitative trend is reported by Guo and Sung (1997) in an empty tube. The trend of Nusselt number with Womersley number is also shown not to be monotonic. To better consider this effect, Fig. 12 is plotted in which variation of average Nusselt number against Womersley number is shown for three different conditions with the same thickness of porous layer.

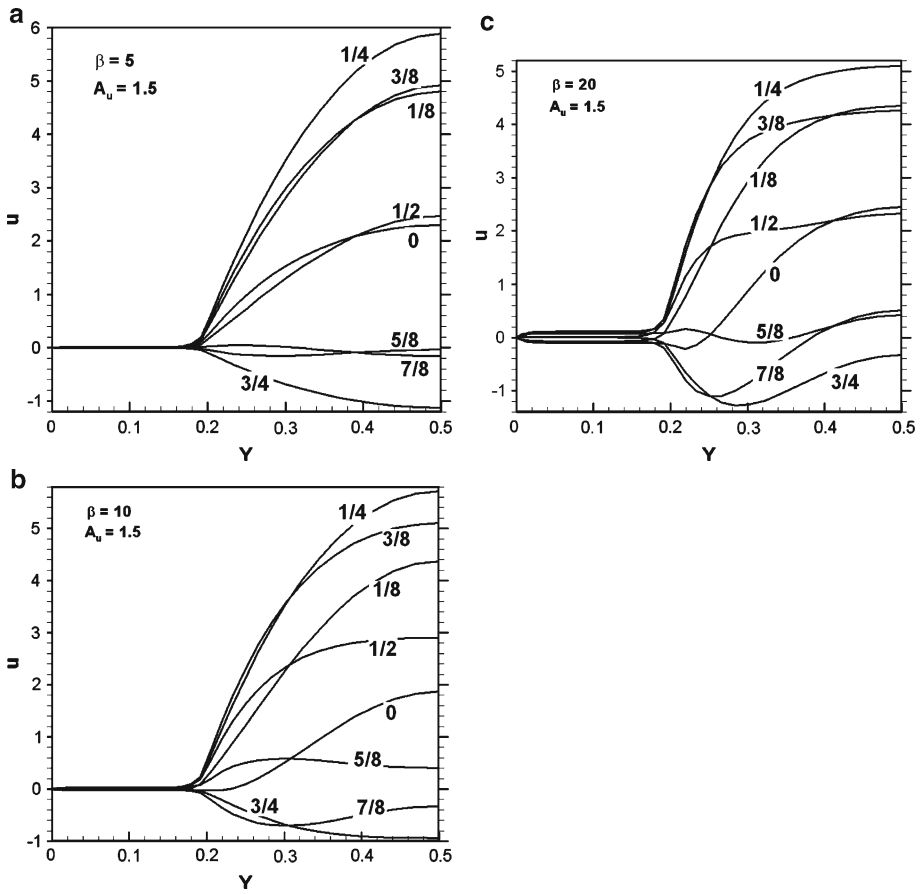

Fig. 13 Comparison of velocity profiles in eight different times in a period; $A_u = 1.5$, **a** $\beta = 5$, **b** $\beta = 10$, and **c** $\beta = 20$ (curves are labeled with the ratio of their phase divided by 2π)

Figure 12 shows that Nusselt number has a minimum around $\beta = 10$ when the amplitude is equal to 1.5; however, even in this minimum point, average pulsatile Nusselt number is greater than steady Nusselt number. Effect of thermal conductivity ratio and Biot number is also studied in Fig. 12. It is clear that Biot number does not have a major effect on normalized Nusselt number in pulsating flow. In other words, the ratio of Nusselt numbers in pulsatile and steady flows are not significantly influenced by departure from LTE condition; whereas the decrease of k_{sf} from 100 to 1 leads to a considerable fall in normalized pulsatile Nusselt number. It may be implied that thermal conduction of solid phase in porous media contributes to augmentation of Nusselt number in pulsatile flow. To summarize, based on Figs. 11 and 12 it can be argued that when Womersley number is low enough, Nusselt number increases monotonically with amplitude. However, in larger amplitudes, Nusselt number remains stable when A_u is smaller than one, and surges around this value of amplitude. At certain amplitude, Nusselt number is high in relatively great or small frequencies, and reaches a minimum value in a certain frequency depending on the amplitude.

To get an idea about the above-mentioned trends, varying velocity and temperature profiles are plotted in tree different Womersley numbers in Figs. 13 and 14. It is shown in Fig. 14

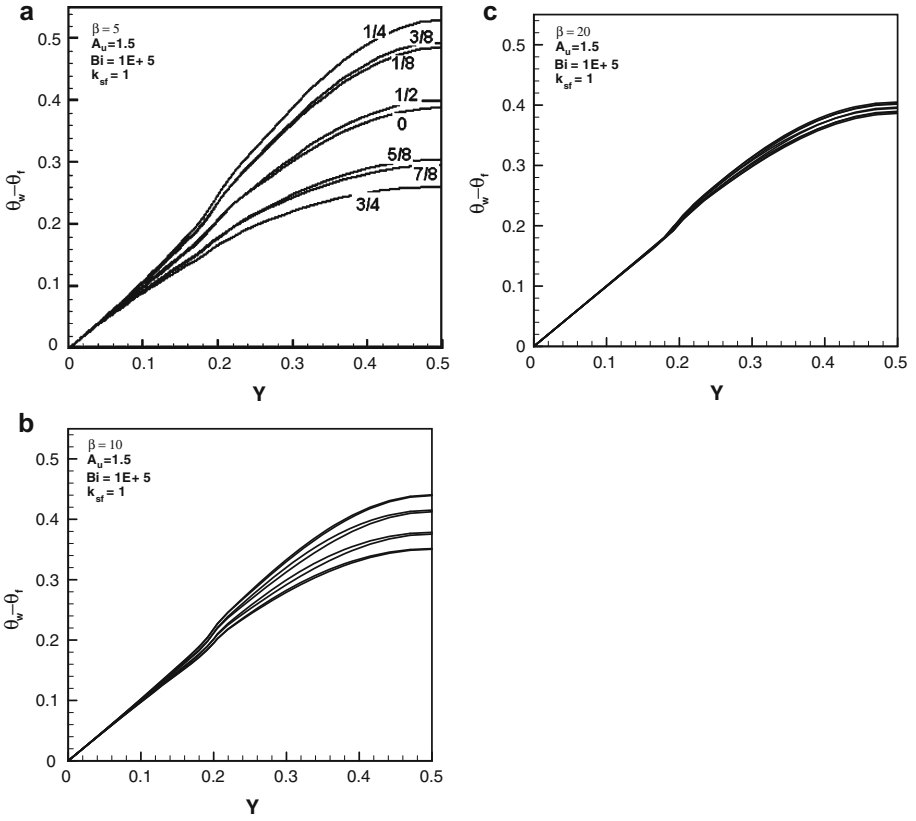

Fig. 14 Comparison of unsteady temperature profiles in eight different times in a period; $A_u = 1.5$, **a** $\beta = 5$, **b** $\beta = 10$, **c** $\beta = 20$ (in the first figure, curves are labeled with the ratio of their phase divided by 2π)

that as Womersley number increases, fluctuations in fluid temperature are stabilized. In other words variation of fluid velocity is too rapid for temperature to be affected. In contrast, at lower frequencies temperature varies in a wider range.

The velocity profile also depends sensibly on Womersley number (Fig. 13). It is evident that when A_u is greater than unity, reverse flow appears and the absolute value of velocity; however, in high values of Womersley number the forward and backward flow may exist in the same time. It is also observed that in higher frequencies more fluid enters the porous region.

To summarize, when frequency is low, temperature and velocity both fluctuate considerably and nearly considerable phase differences. This regular pulsation leads to enhancement of unsteady Nusselt number defined according to Eqs. 33–35 in relatively low frequencies. An increase in amplitude increases range of fluctuation, but it does not affect the pattern of velocity and temperature profiles. This is the reason why variation of unsteady Nusselt number with amplitude is monotonic in this case. As frequency grows, temperature profiles tent to stabilize, and velocity profiles begin having turning points. The interaction of velocity and temperature fields leads to complicated trends in relatively large frequencies. That Nusselt number begins growing near $A_u = 1$ is definitely relating to presence of backward flow in this case.

5 Conclusion

A numerical analysis is performed on forced convection in a channel partially filled with porous media under LTNE condition. Effects of three determining parameters on steady state Nusselt number are considered; Biot number, as a measure of departure from thermal equilibrium, is assessed, and it is shown that the Nusselt number in smaller values of Biot number is lower. However, the overestimation of LTE assumption is not more than 5% in a typical problem. Solid-to-fluid thermal conductivity is also shown to be important in heat transfer. As this ratio become greater, Nusselt number increases; however, the rate of increase is very low over $k_{\mathrm{sf}} = 100$. Sensibility of Nusselt number to k_{sf} decreases in smaller values of Biot number. The trend of Nusselt number with the thickness of porous media is not monotonic; in small thicknesses it has a negative influence on heat transfer, but as $e/2H$ tends to 0.5 Nusselt number sharply enhances. For pulsating flow, if the modified version of Nusselt number, which is introduced in the previous section, is used, the time-averaged Nusselt number for a pulsatile flow is often greater than that of the steady flow corresponding to its mean pressure gradient. It is also observed that average Nusselt number has a minimum when its variation against Womersley number or frequency is considered. The behavior of velocity and temperature profile in the case of pulsatile flow is somewhat complicated, and although some hints are introduced in this article, more consideration is needed in order to obtain a general theory. It can be a subject for future researches.

References

Abu-Hijleh, B.A., Al-Nimr, M.A., Hader, M.A.: Thermal equilibrium in transient forced convection porous channel flow. Transp. Porous Media **57**, 49–58 (2004)

Alazmi, B., Vafai, K.: Analysis of fluid flow and heat transfer interfacial conditions between a porous medium and a fluid layer. Int. J. Heat Mass Transf. **44**, 1735–1749 (2001)

Alazmi, B., Vafai, K.: Constant wall heat flux boundary conditions in porous media under local thermal non-equilibrium conditions. Int. J. Heat Mass Transf. **45**, 3071–3087 (2002)

Alkam, M.K., Al-Nimr, M.A.: Transient non-Darcian forced convection flow in a pipe partially filled with a porous material. Int. J. Heat Mass Transf. **41**(2), 347–356 (1997)

Alkam, M.K., Al-Nimr, M.A.: Improving the performance of double-pipe heat exchangers by using porous substrates. Int. J. Heat Mass Transf. **42**, 3609–3618 (1999)

Alkam, M.K., Al-Nimr, M.A., Hamdan, M.O.: Enhancing heat transfer in parallel-plate channels by using porous inserts. Int. J. Heat Mass Transf. **44**, 931–938 (2001)

Al-Nimr, M.A., Abu-Hijleh, B.: Validation of thermal equilibrium assumption in transient forced convection flow in porous channel. Transp. Porous Media **49**, 127–138 (2002)

Al-Nimr, M.A., Khadrawi, A.: Transient free convection fluid flow in domains partially filled with porous media. Transp. Porous Media **51**(2), 157–172 (2003)

Amiri, A., Vafai, K.: Analysis of dispersion effects and non-thermal equilibrium, non-Darcian, variable porosity, incompressible flow through porous media. Int. J. Heat Mass Transf. **37**, 939–954 (1994)

Amiri, A., Vafai, K., Kuzay, T.M.: Effects of boundary condition on non-Darcian hrat transfer through porous media and experimental comparison. Numer. Heat Transf. A **27**, 651–664 (1995)

Beavers, G.S., Joseph, D.D.: Boundary condition at naturally permeable wall. J. Fluid Mech. **30**, 197–209 (1967)

Bejan, A.: Convection Heat Transfer. Wiley, New York (1984)

Byun, S.Y., Ro, S.T., Shin, J.Y., Son, Y.S., Lee, D.-Y.: Transient thermal behavior of porous media under oscillating flow condition. Int. J. Heat Mass Transf. **49**, 5081–5085 (2006)

Chatwin, P.C.: On the longitudinal dispersion of passive contaminant in oscillatory flows in tubes. J. Fluid Mech. **71**, 513–527 (1975)

Guo, Z., Sung, H.: Analysis of the Nusselt number in pulsating pipe flow. Int. J. Heat Mass Transf. **4010**, 2486–2489 (1997)

Guo, Z., Kim, S.Y., Sung, H.J.: Pulsating flow and heat transfer in a pipe partially filled with a porous medium. Int. J. Heat Mass Transf. **40**(17), 4209–4218 (1997)

Hooman, K., Ranjbar-Kani, A.A.: A perturbation based analysis to investigate forced convection in a porous saturated tube. J. Comput. Appl. Math. **162**, 411–419 (2004)
Huang, P.C., Vafai, K.: Internal heat transfer augmentation in a channel using an alternate set of porous cavity. Numer. Heat Transf. A **25**(5), 519–539 (1994)
Huang, P.C., Nian, S.H., Yang, C.F.: Enhanced heat-source cooling by flow pulsation and porous block. J. Thermophys. Heat Transf. **19**(4), 460–470 (2005)
Jeng, T.M., Tzeng, S.C., Hung, Y.H.: An analytical study of local thermal equilibrium in porous heat sinks using fin theory. Int. J. Heat Mass Transf. **49**, 1907–1914 (2006)
Jiang, P.X., Ren, Z.P., Wang, W.X., Wang, Z.: Forced convective heat transfer in a plate channel filled with solid particles. J. Therm. Sci. **5**, 43–53 (1996)
Jiang, P.X., Ren, Z.P.: Numerical investigation of forced convection heat transfer in porous media using a thermal non-equilibrium model. Int. J. Heat Fluid Flow **22**, 102–110 (2001)
Kaviany, M.: Laminar flow through a porous channel bounded by isothermal parallel plates. Int. J. Heat Mass Transf. **28**, 851 (1985)
Khadrawi, A.F., Tahat, M.S., Al-Nimr, M.A.: Validation of the thermal equilibrium assumption in periodic natural convection in porous domains. Int. J. Thermophys. **26**(5), 1633–1649 (2005)
Khashan, S.A., Al-Nimr, M.A.: Validation of the local thermal equilibrium assumption in forced convection of non-Newtonian fluids through porous channels. Transp. Porous Media **61**, 291–305 (2006)
Khashan, S.A., Al-Amiri, A.M., Al-Nimr, M.A.: Assessment of the local thermal non-equilibrium condition in developing forced convection flows through fluid-saturated porous tubes. Appl. Therm. Eng. **25**, 1429–1445 (2005)
Kim, S.J., Jang, S.P.: Effects of the Darcy number, the Prandtl number, and the Reynolds number on local thermal non-equilibrium. Int. J. Heat Mass Transf. **45**, 3885–3896 (2002)
Klien, H., Eigenberger, G.: Approximate solution for metallic regenerative heat exchangers. Int. J. Heat Mass Transf. **44**, 3553–3563 (2001)
Kuznetsov, A.V., Nield, D.A.: Forced convection with laminar pulsating counterflow in a saturated porous channel. Transp. Porous Media **77**, 447–462 (2009)
Leong, K.C., Jin, L.W.: An experimental study of heat transfer in oscillating flow through a channel filled with an aluminum foam. Int. J. Heat Mass Transf. **48**, 243–253 (2005)
Marafie, A., Vafai, K.: Analysis of non-Darcian effects on temperature differentials in porous media. Int. J. Heat Mass Transf. **44**, 4401–4411 (2001)
Mohamad, A.A.: Heat transfer enhancements in heat exchangers fitted with porous media Part I: constant wall temperature. Int. J. Therm. Sci. **42**, 385–395 (2003)
Nield, D.A.: Effect of local thermal non-equilibrium in steady convective processes in a saturated porous media: forced convection in a channel. J. Porous Media **1**, 181–186 (1998)
Nield, D.A., Kuznetsov, A.V.: Forced convection with laminar pulsating counterflow in a saturated porous channel. ASME J. Heat Transf. **131**, 101005 (1–8) (2009)
Nield, D.A., Kuznetsov, A.V., Xiong, M.: Effect of local thermal non-equilibrium on thermally developing forced convection in a porous medium. Int. J. Heat Mass Transf. **45**, 4949–4955 (2002)
Nield, D.A., Kuznetsov, A.V., Xiong, M.: Thermally developing forced convection in a porous medium: parallel plate channel with walls at uniform temperature, with axial conduction and viscous dissipation effects. Int. J. Heat Mass Transf. **46**, 643–651 (2003)
Pavel, B.I., Mohamad, A.A.: An experimental and numerical study on heat transfer enhancement for gas heat exchangers fitted with porous media. Int. J. Heat Mass Transf. **47**, 939–4952 (2004)